J2.4 TOWARDS A FUNDAMENTALLY NEW UNDERSTANDING OF THE MARINE ATMOSPHERIC BOUNDARY LAYER

Ann-Sofi Smedman*[1)], U. Högström[1)], X. Guo Larsén[2)], C. Johansson[1)], A. Rutgersson[1)], A. Sjöblom[1)], K.K. Kahma[3)] and H. Pettersson[3)]
[1)]Uppsala University, Uppsala, Sweden; [2)]Risø National Laboratories, Roskilde, Denmark; [3)]Finnish Institute of Marine Research, Helsinki, Finland

1. INTRODUCTION

Accurate parameterization of the turbulent exchange of momentum, sensible and latent heat at the surface of the ocean is of fundamental importance for numerical climate prediction and weather forecasting. Based on data from ships and near-shore platforms schemes have been developed for parameterization of the fluxes in terms of so called 'bulk parameters', i.e. wind speed near the surface of the ocean, surface temperature and temperature and humidity at a near-surface reference height. DeCosmo et al. (1996) report results from the HEXOS experiment, at a North Sea platform; Fairall et al. (1996) from the tropical Pacific (the TOGA COARE experiment); Mahrt et al (1996) from Danish coastal waters (Vindeby) etc.

A close look at the results of these studies reveal large data scatter and even apparent inconsistencies in results. It is obvious from other recent studies, which specifically include measurements of the wave field, Donelan et al. (1997), Drennan et al. (1999), Rieder and Smith (1998) and our own studies (see below), that effects from waves are of fundamental importance for the turbulent exchange processes in the marine boundary layer and should be included in parameterizations in models.

This contribution summarizes results from measurements during an eight-year period (May, 1995 – present) at the air-sea interaction station Östergarnsholm in the Baltic Sea. It illustrates vividly that the 'classical' concept of the sea surface as an analogue to a solid surface with moving roughness elements is valid only for the much studied case of growing waves and that understanding the role of relatively long waves, which travel faster than the wind, is crucial for a correct treatment of the air-sea exchange processes.

2. SITE AND MEASUREMENTS

The measurements analysed in this paper have been made at the Östergarnsholm station for air/sea interaction research. It consists of an instrumented 30 m high tower situated at the southernmost peninsula of the low island Östergarnsholm, 4 km east of the big island Gotland in the Baltic sea, Figure 1, and measurements with a 3D Waverider buoy moored at 36 m depth about 4 km to the south-east of the tower. The instruments on the tower include eddy correlation measurements with Solent 1012R2 sonic anemometer (Gill Instruments, Lymington, United Kingdom) at 8, 16 and 24 m above the ground and slow response, 'profile' sensors for wind speed and direction (light-weight cup anemometers and Styrofoam wind vanes) and temperature at 5 levels. The base of the tower is situated 1 – 2 m above the sea level, the actual level changing over time, as a result of the prevailing wind conditions over the Baltic Sea and parts of adjacent North Sea areas. Actual measuring heights above the sea level are derived from a sea level record at Visby, situated on the west coast of Gotland.

* *Corresponding author address:* Ann-Sofi Smedman, Dept. of Earth Sciences, Meteorology, Uppsala Univ., Villavägen 16, 75236 Uppsala, Sweden, e-mail: Ann-Sofi Smedman@met.uu.se

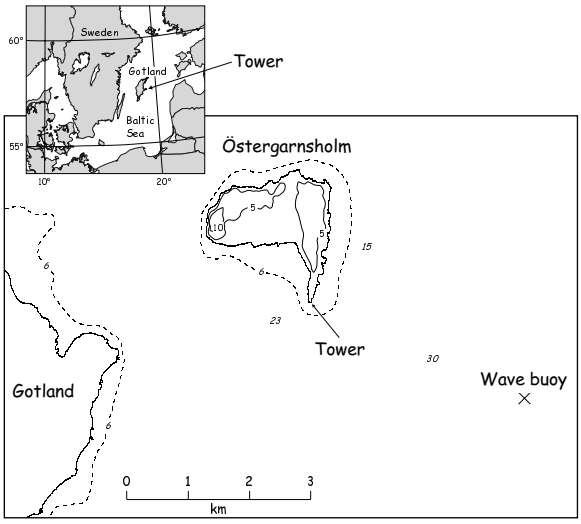

Figure 1. Map of the Baltic Sea, with a close-up of Östergarnsholm. The location of the wave buoy is also included.

The sonic anemometers have been calibrated in a big wind tunnel, resulting in individual flow distortion correction matrices (Grelle and Lindroth,1994). Also the cup anemometers have been individually calibrated in this big wind tunnel. Repeated calibrations of both types of anemometers after about a year of service in the field show very good reproducibility of the calibration results. In the field, turbulence data are recorded at 20 Hz. From the sonic signals the three orthogonal components of the wind and virtual temperature (the measured temperature signal agrees to within 0.2% with the virtual temperature, Dupuis et al., 1997) are obtained. Turbulence statistics, such as variances, co-variances and spectra are calculated as 60-minute averages. 'Profile' variables are measured with 1 Hz and averaged over 60-minute periods as well. Wave measurements were recorded once in an hour. The directional spectrum is calculated from 1600 s vertical, north and west displacement time series on board the buoy following the method presented by Longuet-Higgins et al. (1963). The spectral variance, mean direction, directional spreading, skewness and kurtosis calculated at 64 frequency bins cover a frequency range of [0.025 0.58]. The significant wave height is calculated by trapezoid method from frequencies between 0.05 and 0.58 Hz and the peak frequency is determined by a parabolic fit to the three frequencies that form the peak of the spectrum.

The meteorological measurements have been running semi-continuously since May, 1995. Wave-data have been recorded semi-continuously during the same period but with breaks during wintertime periods with risk for ice damage.

For winds coming from the sector 80 – 220 degrees, there is undisturbed over water fetch for more than 150 km, and only data with this wind direction have been used here. About 10 km from the peninsula, the depth is 50 m, reaching below 100 m farther out. In Smedman et al. (1999), the possible influence of limited water depth on the tower measurements was studied in detail. Flux footprint calculations were done, showing that the turbulence instruments "see" areas far upstream of the island. Waves up to 5 s wave period are deep water waves in the footprint of the top level. Longer waves begin to feel the bottom and their phase speed is reduced. According to Anctil and Donelan (1996), up to rather long wave periods, the only significant effect of steepening of shoaling waves is a change in phase speed. Taking the 'footprint weighting function' $F(z)$ from Eq.(A7) of the Appendix of Smedman et al. (1999), it is possible to calculate a weighted mean phase speed

$$\left\langle c_p \right\rangle = \int_0^\infty F(x,z) c_p(x) dx \qquad (1)$$

Here the peak wave phase speed c_p was iterated from the dispersion relation

$$c_p = \frac{g}{\omega_0} \tanh\left(\frac{\omega_0 h}{c_p}\right) \qquad (2)$$

where h is the water depth, ω_0 the peak wave frequency and g acceleration of gravity. Hereafter whenever we will use "c_p" we mean the weighted mean $\langle c_p \rangle$. As will be demonstrated below, measurements for growing wave conditions at Östergarnsholm give results in excellent agreement with corresponding results obtained in oceanic conditions at deep water and far from land. This gives additional credence for our claim that the measurements at this site are likely to represent the structure of the marine boundary layer for open sea conditions in most cases.

3. CRITERIA FOR CHARACTERIZING SEA STATE

On dimensional grounds, Charnock, (1955) derived the following expression for the roughness of the sea

$$z_0 = \alpha u_*^{\,2} / g \qquad (3)$$

where α is the so-called Charnock parameter or dimensionless roughness and g is acceleration of gravity. Eq. (3) is often used in large-scale

synoptic and climatic models with a constant value for α, typically in the range 0.01 – 0.03. For *pure wind seas*, several investigations have, however shown that α is a function of wave age, defined as

$$c_p/u_* \qquad (4),$$

where c_p is the phase speed of the waves at the peak of the spectrum. That this is indeed the case has convincingly been demonstrated by Komen et al. (1998).
Drennan et al. (2003) have gathered data from five field experiments with pure wind sea, defined as

$$E(\textit{wind sea}) > 5E(\textit{swell}) \qquad (5),$$

where *E*(*wind sea*) is the part of the two-dimensional wave spectrum identified as pure wind sea and *E*(*swell*) the corresponding part associated with swell. They also require that $u_*/c_p > 0.05$ and that the wave spectra have just one peak. The analysis by Drennan et al. (2003) shows conclusively that z_0 made dimensionless with the standard deviation of surface elevation σ is a function of the wave age alone for

$$E(\textit{swell})/\, E(\textit{wind sea}) \; < 0.2.$$

To parametrize the effect of swell in the simplest possible situation, our selection criteria require that the spectra are single peaked and the dominant waves have the same direction as the wind. In such a wave field even the directional wave spectrum often does not provide clear and unambiguous means to do the standard partitioning to wind sea and swell that was used by Drennan et al. (2003). The fact that wind input to waves is positive only for waves slower than the wind can be used directly to make simpler division of the spectra into two parts:

$$E_1 = \int_0^{n_1} S(n)dn\,, \qquad E_2 = \int_{n_1}^{\infty} S(n)dn$$

$$n_1 = \frac{g}{2\pi U_{10}\cos\theta} \qquad (6)$$

Here *n* is frequency, *S(n)* is the one-dimensional wave spectrum and n_1 is the frequency which corresponds to a phase speed *c* equal to the wind speed U_{10} at 10 m height. One could in principle call E_1 the swell energy and E_2 the wind sea energy. However, to avoid any confusion with the standard partitioning and our division we will hereafter speak about long-wave spectral part, E_1 and a short-wave spectral part E_2.

Figure 2 shows a typical example of spectral analysis of the wave spectra. The four sub-graphs show respectively: *a*, wave direction compared with wind direction (the horizontal line); *b*, the logarithm of $n^4S(n)$; *c*, the spectrum *S(n)*; *d*, comparison of U_{10} (horizontal line), $U_c = U_{10}\cos\theta$, where $\theta = \theta(n)$ is the angle between the wave at frequency *n* and the mean wind and the phase velocity *c*. Thus, E_1 is the area to the left of the vertical line in Figure 2c and E_2 the area to the right of that line. As shown in Smedman et al. (2003), E_2 is proportional to the fourth power of the wind speed at 10 m, whereas there is no relation at all between E_1 and the wind speed.

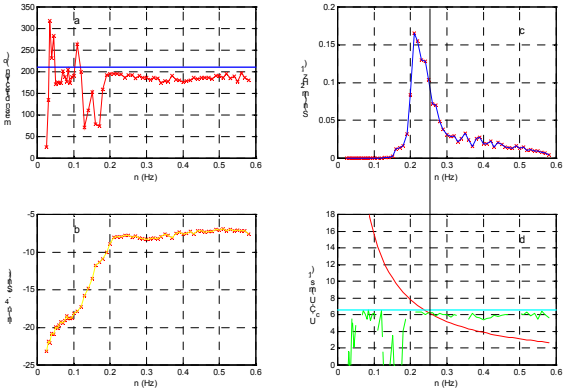

Figure 2. Example of wave spectral information from one particular hour (1999 06 02 07h). Subplot a) Wave direction as a function of frequency, n; also shown is the mean wind direction. Subplot b) $\ln\{n^4S(n)\}$ *as a function of n. Subplot c) Spectrum S(n) as a function of n. d) Phase velocity, c, mean wind speed at 10 m, U, and* $U_c = U\cos\theta$, *where* θ *is the angle between the wind and the wave, all plotted against n; the vertical line represents the frequency where c = U_c. This line, which continues up to subplot c) is the basis for division of the spectrum into two parts: E_1, representing waves that travel faster than the wind speed at 10 m ('long waves') and E_2, representing slower waves ('shorter waves'). From Smedman et al. (2003a).*

Table 1 shows the various parameters used in the Östergarnsholm studies for characterizing sea state and approximate limits for the categories 'growing sea', 'mixed sea' and 'swell' respectively for the parameters.

	c_p/u_*	c_p/U_{10}	E_1/E_2
Growing sea	< 20	< 0.8	< 0.1
Mixed sea	20 - 30	0.8 – 1.2	0.2 - 4
Swell	> 30	> 1.2	> 4

Table 1. Overview of sea state parameters used in this contribution with approximate limits for 'growing sea', 'mixed sea' and 'swell' respectively.

4. RESULTS

4.1 *Overview*

Our findings are summarized in a schematic manner in Table 2, which lists characteristics of the marine atmospheric boundary layer (MABL) into four categories of stability and sea state.

Stability: Waves:	***Unstable and neutral Growing waves***	***Unstable and neutral Mixed sea***	***Unstable and neutral Swell***	***Stable Minor influ-ences of waves***
Stability parameter z/L, Ri	Same as over land, M-O theory valid	Increasing influence of waves through decreasing u_*	Not valid	Can be used
Mechanic turbulence structure	Same as over land, M-O: theory valid log-law valid; z_o function of u_*/c_p	Φ_m decreases decreasing influence of z z_o increasing func. of wave state: u_*/c_p and E_1/E_2 log-law not valid	$\Phi_m \cong 0$ z_i scaling, log-law not valid; inactive turbulence dominates	Decreased transport through shear sheltering
Thermal turbulence structure	Same as over land, M-O theory valid	z_{oT} const. C_{HN}= 1.0 for U<10 m/s Spray effect for U>10 m/s	Frictional decoupling at surface	Decreased transport through shear sheltering
Energy spectra	Same as over land $(S_w/S_u)_{iner.subr.}$ =1.33	High and low freq. modification $(S_w/S_u)_{iner\ subr}$ decreasing	Resemble free convection spectra $(S_w/S_u)_{iner.sur}$ =1.1	Strong influence of low-level jets

Table 2. Schematic overview of new concept of the marine boundary layer, schematically divided into four combinations of atmospheric stability and sea state ('waves').

The results corresponding to the various boxes in Table 2 are discussed in Sub-sections 4.2 – 4.5 below.

4.2 *Basic characterization of the state of the MABL and the characteristics of the neutral MABL*

As discussed later, the MO-parameter *z/L* is found to be a complicated mixture of stability in a proper sense and wave influences in the MABL. As a basic criterion of atmospheric stability, we therefore simply adopted the sign of the flux of virtual potential temperature at the surface in Smedman et al. (2003a) and other papers. For neutrality we adopted in that paper the criterion that the magnitude of the heat flux is below a certain limit and wind speed above some chosen value. Analysis of that data subset revealed convincingly that neutrality is not a sufficient criterion for a logarithmic wind law to ensue. As illustrated in Figure 3, a true logarithmic wind law ensues only for $E_1/E_2 < 0.05$, the curve deviating gradually more and more from a straight line in the lin-log representation for increasing values of E_1/E_2.

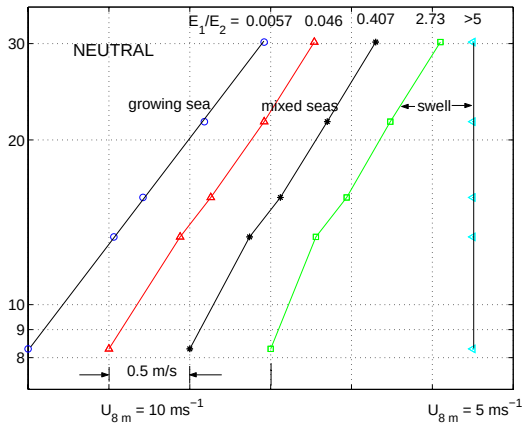

Figure 3. Mean wind profiles in lin-log representation for neutral conditions (1077 hours of data), divided into five groups according to wave spectral ratio E_1/E_2. Note, that a logarithmic profile is only obtained for E_1/E_2 = 0.0057.

A similar criterion was also adopted for defining growing sea. For this data subset, the roughness length z_0 divided by the standard deviation of surface elevation, σ was plotted as a function of inverse wave age u_*/c_p, where u_* is friction velocity and c_p is the wave speed at the spectral maximum. Drennan et al. (2003) show that data for growing sea gathered from several oceanic experiments collapse in this representation, and it was very satisfactory to find that our Östergarnsholm data did so as well, Figure 4. It is clear from that figure that our regression line in this representation (log z_0/σ against log u_*/c_p), the solid line, and the corresponding regression line of Drennan et al. (2003), dashed line, come quite close.

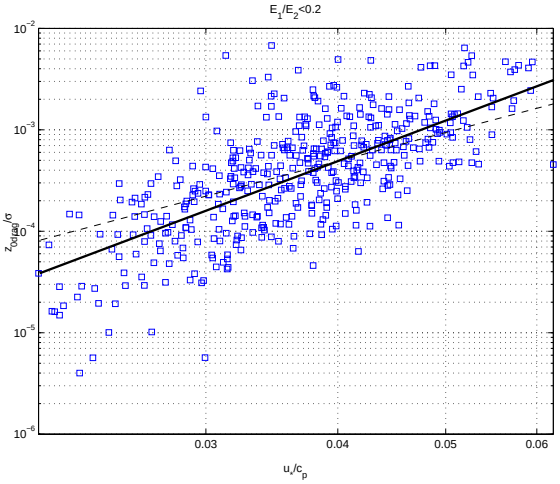

Figure 4. Dimensionless roughness length z_0/σ, where σ is the RMS surface elevation, plotted on a logarithmic scale against the inverse wave age parameter u_*/c_p for neutral conditions and growing sea, defined here as $E_1/E_2 < 0.2$. Solid line: regression of Östergarnsholm data; dashed line: Regression by Drennan et al. (2003), based on data from several measurements over the open ocean: $z_0/\sigma = 13.3(u_*/c_p)^{3.4}$.

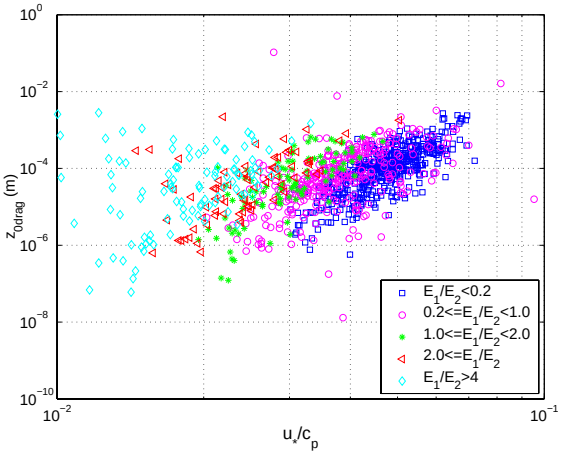

Figure 5. Apparent roughness length derived from inserting measured values of u_* and U_{10} in the logarithmic wind law, plotted against u_*/c_p. Data have been divided according to E_1/E_2, see insert legend.

Plotting the drag coefficient C_D or, which amounts to basically the same thing, the 'apparent roughness length', which is derived from measurements of wind speed and friction velocity at 10 m and *assuming* a logarithmic profile down to the surface, against u_*/c_p for the general neutral case, clearly showed that a significant ordering of the data in bands according to E_1/E_2 occurs, i.e. the wave influence is governed by two independent parameters, u_*/c_p and E_1/E_2, Figure 5.

4.3 *Unstable conditions, swell and inactive turbulence*

It was demonstrated in Smedman et al. (1999) that during conditions of pronounced swell having roughly the same direction as the near-surface wind, the flux of momentum at the surface is strongly reduced, giving consequently a small value for u_*. This was shown to be due to upward transport of momentum by the long waves. The shorter waves still produce some drag, causing an 'ordinary' downward transport of momentum. Sometimes the upward transport dominates, so that the net transport is positive. This means that even for cases with a small positive heat flux, the value of $-L$, where L is the Obukhov length will also be small, giving large negative values of z/L in the unstable surface layer, see Rutgersson et al. (2001).

In an earlier study in similar conditions, based on a combination of airborne and tower-mounted measurements, Smedman et al. (1994), it was shown that turbulence of boundary-layer scale was produced at the top of the unstable boundary layer (at around 1000 m) and brought down to the surface layer by the pressure transport term (obtained as the residual), Figure 6.

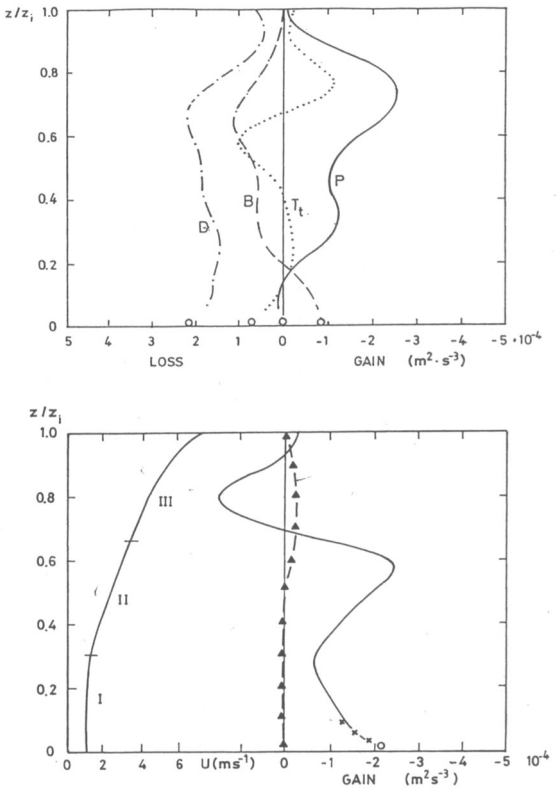

Figure 6. Turbulence energy budget of Smedman et al. (1994). (a) Mean profiles of the various terms of the turbulence energy budget that were directly derived from the airborne slant profiles (curves) and mast measurements (circles), with notation: P = mechanical production; B = buoyancy production; T_t = turbulent transport of turbulent energy; D = dissipation. (b) Right-hand part: imbalance obtained when summing up the directly measured terms. Solid line: aircraft slant profile mean; dashed line with crosses: data from horizontal flight legs; circles: mast data. Dashed curve with triangles is the time rate of change term derived from measurements 1½ hour apart. Left hand part: Mean wind profile.

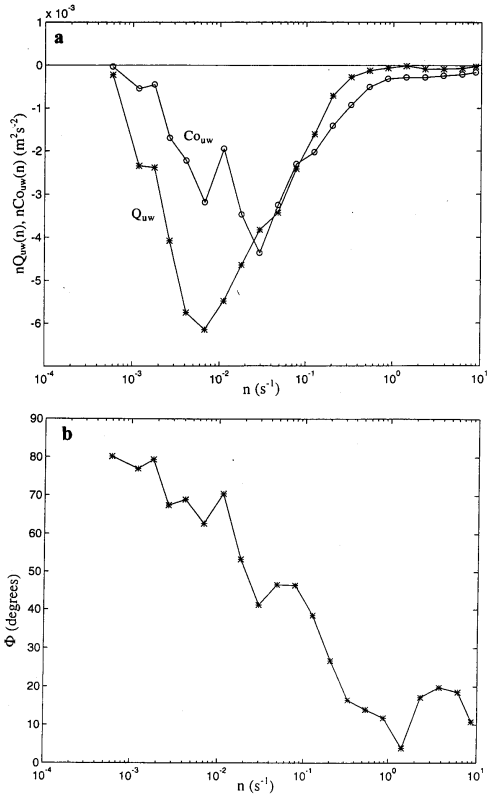

Figure 7.(a) Mean u, w cospectra (curves with circles) and quadrature spectra (curves with stars) for September 18, 1995 at Östergarnsholm, 10 m, and (b) the correspon-ding phase angle ϕ as a function of frequency. From Smedman et al. (1999).

In the surface layer it contributed to the turbulence level but not to the shearing stress, Figure 7, leading thus to excessive values of dimensionless standard deviation of the wind components and to substantial reduction of the correlation coefficient $-r_{uw}$, Figure 8. It was concluded that this mechanism is identical to Townsend's (1961) 'inactive' turbulence. Analysis of the turbulence kinetic energy budget in Rutgersson et al. (2001) gave the same conclusion: energy was brought down from higher layers into the surface layer by the pressure transport term. In Sjöblom and Smedman (2002) and Sjöblom and Smedman (2003) it was confirmed from an extensive data set from Östergarnsholm that when stratification is unstable, this is a general feature.

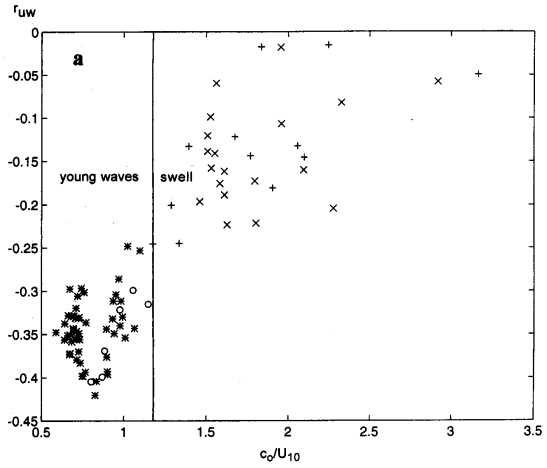

Figure 8. Correlation coefficient $r_{uw} = \overline{u'w'}/(\sigma_u \sigma_w)$ for 10 m plotted as a function of the wave age parameter c_0/U_{10}, where c_0 is peak wave frequency (same as c_p) during the time period 14 – 19 September, 1995. The different symbols refer to different measuring days. FromSmedman et al. (1999).

As discussed in Smedman et al. (1994) and in Rutgersson et al. (2001), in spite of the fact that the heat flux may be quite small, the turbulence structure of the unstable MABL when swell is occuring resembles that of a BL in the state of free convection, giving spectra that scale with the depth of the entire convective boundary layer, z_i. In Johansson et al. (2001) it was demonstrated that other surface layer characteristics as well scale with z_i/L in the unstable boundary layer over land, Figure 9. A very similar result was reported from Östergarnsholm, Johansson (2003). It was also demonstrated that the temperature structure of the unstable marine surface layer seems not to follow MO scaling.

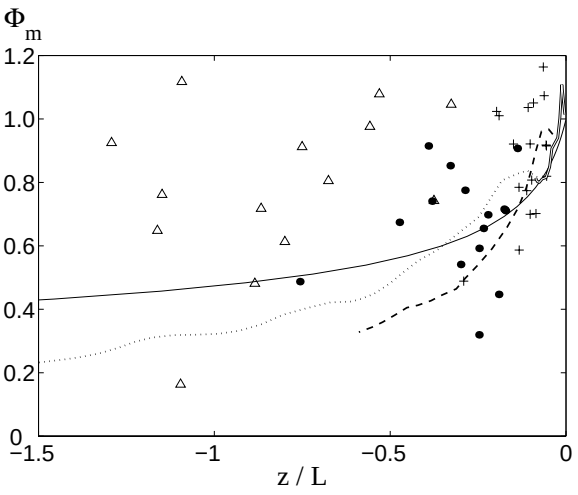

Figure 9. Plot of ϕ_m against z/L for measurements in three z_i/L-ranges, where z_i is the height of the convective boundary layer: pluses, -0.5 > z_i/L >-5; filled circles, -25 > z_i/L >-35; and triangles, z_i/L< -60. The thin line is from Högström (1996). The other lines are from large-eddy simulations of Khanna and Brasseur (1997): double line, z_i/L = -0.44; dashed line, z_i/L = -3; dotted line, z_i/L = -8. From Johansson et al. (2001).

Wind component spectra in the unstable MABL are very sensitive to the wave state, Smedman et al. (2003b). The wave signal is clearly seen as a peak in spectra for the vertical component; the wave influence is transferred to the horizontal component spectra and to higher frequencies by the cascade process. This may result in –5/3 slope at high enough frequency, but the ratio S_w/S_u is found to be around 1.0 or 1.1 instead of 1.3 as predicted for local isotropy for all cases of mixed seas or swell. It was also demonstrated that for growing sea and near-neutral conditions, wind component spectra are identical to those found during similar conditions over land, Högström et al. (2002), including having the predicted 4/3 ratio for S_w/S_u in the inertial subrange, Figure 10.

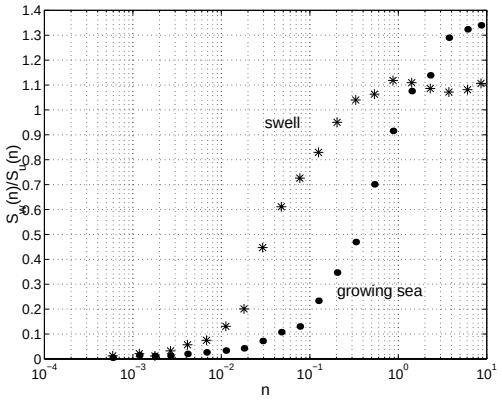

Figure 10. The spectral ratio $S_w(n) / S_u(n)$ plotted as a function of frequency n. The two curves are each based on measurements during 4 consecutive hours. The data denoted 'growing sea' (dots) is from 15 September, 1995 and has c_0/U = 0.7; the curve denoted 'swell' (stars) is from 18 September, 1995 and has c_0/U = 2.3. The growing sea data are seen to reach the predicted value for local isotropy, 4/3 at around n = 5 Hz, whereas the swell data level out around 1.1 for n > 1 Hz. From Smedman et al. (2003b).

4.4 General features of the stable MABL at Östergarnsholm

In Smedman et al. (1997) it was demonstrated that sometimes when the atmospheric stratification is stable, a regime with 'quasi-frictional decoupling' occurs at Östergarnsholm. A later study, Smedman et al. (2004), has identified a physical mechanism which explains this phenomenon, called 'shear sheltering'. It occurs when there is a low-level wind maximum present near the surface (at between 40 and 300 m above the water surface). As shown by Hunt and Durbin (1999), a layer with strong vorticity, like a low-level jet, prevents eddies of a certain size range to penetrate from higher layers in the boundary layer down to the surface, thus reducing both turbulent transport and turbulence intensity in the stable surface layer. Figure 11 thus illustrates how low-frequency energy of the longitudinal velocity spectrum is suppressed for cases with a low-level jet compared to cases without such jets. Low-level jets are shown to be a very common phenomenon in the Baltic Sea during the season when the surface of the sea is colder than surrounding land. An analogy in space to the well-known nocturnal jet then develops.

When the MABL is stable, very little influence from waves can be seen. As shown in Smedman et al. (1999), there is a rapid change of regime from very slightly unstable to very slightly stable conditions.

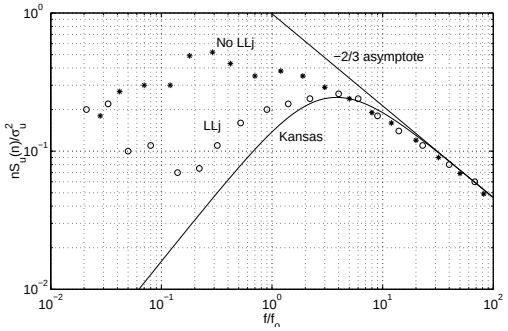

Figure 11. *Normalized mean longitudinal velocity spectrum,* $nS_u(n)/\sigma_u^2$ *plotted against normalized frequency f/f0, where f0 is the frequency of the intercept between the asymptote to the inertial subrange and* $nS_u(n)/\sigma_u^2$ *= 1. The data have been divided into two groups according to the presence of a wind maximum at low height, 'LLJ' or absence of such a maximum, 'No LLJ'. Also included is the curve suggested by Kaimal et al (1972), their Eq. (23). The 'LLJ-spectrum' is the mean of 118 half-hour spectra from 8m at Nässkär for which 300m> h >40m; the 'NoLLJ-spectrum' is the mean of 56 half-hour spectra for cases with no low-level wind maximum. From Smedman et al. (2004).*

4.5 *The exchange of sensible heat and water vapor*

See paper J2.4 by Sahlée et al. (2004).

5. CONCLUSIONS

The Östergarnsholm air-sea interaction research project has led to fundamentally new understanding of the marine atmospheric boundary layer, MABL, and the exchange process at the surface of the ocean:

1. The MABL is very much influenced by the state of the sea

2. For growing sea, i.e. young waves travelling slower than the wind, the turbulence structure in the MABL resembles the boundary layer over land and MO theory is applicable.

3. As soon as some waves are travelling faster than the wind, mature sea or mixed sea, the MABL starts to deviate from the boundary layer (BL) over land.

4. For swell conditions, when long waves travelling faster than the wind dominate, the MABL is quite different from the BL over land.

REFERENCES

Anctil, F. and M.A. Donelan, 1996: Air-Water momentum flux observations over shoaling waves. *J. Phys. Oceanogr.,* **26**, 1344-1353,

Charnock, H., 1955: Wind stress on a water surface. *Q.J.Roy.Met.Soc.*, **81**, 639 – 640.

DeCosmo, J., K.B. Katsaros, S.D. Smith, R.J. Anderson, W.A. Oost, K. Bumke and H. Chadwick, 1996: Air-sea exchange of water vapor and sensible heat: The Humidity Exchange Over the Sea (HEXOS) results, *J. Geophys. Res*., **101**, 12,001 - 12,016.

Donelan, M.A., W.M. Drennan and K.B. Katsaros, 1997: 'The air-sea momentum flux in conditions of wind sea and swell'. *J. Phys. Ocean*., **27**, 2087 - 2099.

Drennan, W.M., K.K. Kahma and M.A.Donelan,1999: On momentum flux and velocity spectra over waves. *Boundary-Layer Meteorology,* **92**, 489 – 515.

Drennan, W.M., H.C. Graber, D. Hauser and C. Quentin, 2003: On the wave age dependence of wind stress over pure sea. *J. Geophys. Re*s., 10.1029/2000JC00715.

Dupuis, H., P.K.Taylor, A.Weil and K. Katsaros, 1997: Inertial dissipation method applied to derive turbulent fluxes over the ocean during the SOFIA/ASTEX and SEMAPHORE experiments with low to moderate wind speeds. *J. Geophys. Res.,* **102**, 21,115-21,129.

Fairall, C.W., E.F. Bradley, D.P. Rogers, J.B. Edson and G.S. Young, 1996: 'Bulk parameterization of air-sea fluxes for TOGA-COARE.'*J. Geophys. Res*., **101,** 3747 - 3764.

Grelle, A. and A. Lindroth, 1994: Flow distortion by a Solent sonic anemometer: Wind tunnel calibration and its assessment for flux measurements over forest and field. *J. Atmos. Oceanic Technol.,* **11**, 1529-1542.

Högström, U., 1996: Review of some basic characteristics of the atmospheric surface layer. *Boundary-Layer Meteorology,* **78**, 215 – 246.

Högström, U., Hunt, J.C.R. and Smedman, A., 2002: 'Theory and measurements for turbulence spectra and variances in the atmospheric neutral surface layer'. *Boundary-Layer Meteorol.,* **103**, 101-124.

Hunt, J.C.R. and P.A. Durbin, 1999: Perturbed vortical layers and shear sheltering. *Fluid Dyn. Res.,* **24**, 375-404.

Johansson, C., A. Smedman, U. Högström, J.G. Brasseur and S. Khanna, 2001: Critical test of Monin-Obukhov similarity during convective conditions. *J. Atm. Sci*., **58**, 1549-1566.

Johansson, C.2003: Influence of external factors on the turbulence structure in the boundary layer. *Comprehensive Summaries of Uppsala Diossertations from the Faculty of Sciences and Technology,* **792,** ACTA UNIVERSITATIS UPSALIENSIS. 34 pp.

Kaimal, J.C., J.C. Wyngaard, Y. Izumi and O.R. Coté, 1972: Spectral characteristics of surface-layer turbulence. *Quart. J. Roy. Met. Soc.,* **98**, 563 – 589.

Khanna, S and J.G. Brasseur, 1997: Analysis of Monin-Obukhov similarity from large-eddy simulation. *J. Fluid Mech.*, **345**, 251-286.

Komen, G, P.A.E.M. Jansen, V.Makin and W. Oost, 1998: On the sea state dependence of the Charnock parameter. *The Global Atmosphere and Ocean System,* **5**, 367-388.

Longuet-Higgins, M.S., D.E. Cartwright and N.D. Smith, 1963: Observations of the directional spectrum of sea waves using the motion of a floating buoy. Ocean wave spectra, *Proc. Nat. Acad. of Science*, *USA*, 111-132.

Mahrt, L., D. Vickers, J. Howell, J. Højstrup, J.M. Wilczak, J. Edson and J. Hare, 1996: 'Sea surface drag coefficients in the Risø Air Sea Experiment'. *J. Geophys. Res*., **101**, 14,327 - 14,355.

Rieder, K.F. and J.A. Smith, 1998: Removing wave effects from the wind stress vector. *J. Geophys. Res.,* **103**, No C1, 1363-1374.

Rutgersson, A., A. Smedman and U. Högström, 2001: The use of conventional stability parameters during swell. *J. Geophys. Res.,* **106**, 27,117-27,134.

Sjöblom, A. and A. Smedman, 2002 : The turbulent kinetic energy budget in the marine atmospheric surface layer. *J. Geophys. Res.,* **107**, doi:10.1029/2001JC 00101016.

Sjöblom, A. and A. Smedman, 2003: Vertical structure in the marine atmospheric boundary layer and its implication for the inertial dissipation method. *Boundary-Layer Meteorology*, **109**, 1-25.

Smedman, A., M. Tjernström and U. Högström, 1994: The near-neutral marine atmospheric boundary layer with no surface shearing stress: a case study. *J. Atm. Sci.*, **51**, 3399 - 3411.

Smedman, A., U. Högström and H. Bergström, 1997: The turbulence regime of a very stable marine airflow with quasi-frictional decoupling. *J. Geophys. Res.*, **102**, 21049-21059.

Smedman, A., U. Högström, H. Bergström, A. Rutgerson, K.K. Kahma and H. Petterson, 1999: A case study of air-sea interaction during swell conditions. *J. Geophys. Res.,***104**, 25,833-25,851.

Smedman, A., X. Guo-Larsén, U. Högström, K. Kahma, and H. Pettersson, 2003a: Effect of sea state on the momentum echange over the sea during neutral conditions. *J. Geophys. Res.*, **108 (C11)** 3367, doi: 10.1029/2002JC001526.

Smedman, A., U. Högström and A. Sjöblom, 2003b: A note on velocity spectra in the marine boundary layer. *Boundary-Layer Meteorol*., **109**, 27-28.

Smedman, A., J. Hunt and U. Högström, 2004: Effects of shear sheltering in a slightly stable atmospheric boundary layer with strong shear.*Quart. J. Roy. Met. Soc.*, **130**, 31-50.

Townsend, A.A., 1961: Equilibrium layers and wall turbulence. *J. Fluid Mech.*, **11**, 97-120.